ARTICLE

Microencapsulation of UV-Curable Self-healing Agent for Smart Anticorrosive Coating

Dong Zhao[a], Mo-zhen Wang[a*], Qi-chao Wu[b], Xiao Zhou[b], Xue-wu Ge[a]

a. CAS Key Laboratory of Soft Matter Chemistry, Department of Polymer Science and Engineering, University of Science and Technology of China, Hefei 230026, China
b. Guangdong Tianan New Material Co., Ltd., Foshan 528000, China

(Dated: Received on May 10, 2014; Accepted on May 20, 2014)

UV-curable polyurethane prepolymer and photoinitiator 1173 were facilely encapsulated in a poly(urea-formaldehyde) shell, which was *in situ* formed by the polymerization of formaldehyde and urea in an oil-in-water emulsion. The diameters of the microcapsules ranged from 118 μm to 663 μm depending on agitation speed, and were obtained via optical microscopy and scanning electron microscopy analyses. The encapsulation percent and the yield of microcapsules prepared at the agitation speed of 600 r/min can reach 97.52wt% and 65.23wt%, respectively. When the water-borne polyurethane (WPU) coating embedded with the prepared microcapsules were scratched, the healing agent could be released from ruptured microcapsules and filled the scribed region. The excellent anticorrosion properties of the WPU coating embedded with the prepared microcapsules were confirmed by the results obtained from both electrochemical impedance spectroscopy and Tafel curves.

Key words: Self-healing, Water-borne polyurethane coating, Corrosion resistance, Poly(urea-formaldehyde) microcapsule, UV-curable coating

I. INTRODUCTION

Corrosive damage of metals is of great complexity and enormous economic importance. A well-known and the most important method for the anticorrosive protection of metal is the application of polymer coatings, which can provide a physical barrier between the metal substrate and corrosive media [1−4]. However, the substrate surface could be still subjected to the attack of corrosive species when the integrity of the coatings was destroyed by the environmental factors, corrosive process occurred on the damaged region. Moreover, the formation and propagation of microcracks in coatings was also accompanied with the significant reduction in the mechanical performance and other properties of the coatings [5]. To remain the anticorrosive protection under the acquired damage, some active containers loaded with corrosion inhibitors have been preembedded into the coatings [6, 7]. Once the coating was damaged and environmentally changed, the loaded corrosion inhibitors can be released accordingly to inhibit the corrosion process of the metals. For instance, ^{1}H-benzotriazole (BTA) and its derivatives are found to be an effective corrosion inhibitor for metals such as copper and mild steel, due to the generation of the complex compound [8, 9]. However, the above method cannot repair the coating damage fundamentally. The risk of corrosion still exists. The mechanical and other damaged properties of the coatings cannot also be healed.

As a matter of course, the concept of "self-healing" attracts the attention of material scientists, who want to fabricate materials with a long-term function [10, 11]. Self-healing materials can be classified into two categories [12]: (i) intrinsic ones that can heal cracks by the materials themselves, and (ii) extrinsic ones, in which foreign healing agent is added after being encapsulated in a container, and then released into the cracks when the coating is damaged. The extrinsic ones have advantages of healing large damaged volume and broad application in most polymeric systems [13]. Generally, a typical extrinsic self-healing system encapsulates two components: active species to form healing material, *i.e*, healing agent and the corresponding catalyst [14−19]. The shell materials for microencapsulation are common resins, such as poly(urea-formaldehyde) (PUF) [20], polyurethane (PU) [21], and polyurea [22]. When the extrinsic self-healing system is mixed with polymer matrix, the healing agent can be released from ruptured microcapsules in damaged area, and solidifies with the help of the catalyst to repair the damage region.

Recently, the concept of catalyst-free extrinsic self-healing system has been proposed. One autonomous, catalyst-free approach should self-heal under natural conditions, such as atmospheric moisture [23, 24], oxygen [25−27], and sunlight [28]. Yang *et al.* reported the microencapsulation of isocyanate monomers, such

*Author to whom correspondence should be addressed. E-mail: pstwmz@ustc.edu.cn, Tel.: +86-551-63600843

as isophorone diisocyanate [29] and hexamethylene diisocyanate [23], based on PU microcapsules through the polymerization of toluene diisocyanate prepolymer and 1,4-butanediol. Isocyanate monomers could react with moisture so as to be used as catalyst-free healing agent. Chung *et al.* introduced PUF microcapsules loaded with healing agents of cinnamide moiety-containing polydimethylsiloxane (CA-PDMS) into enamel paint as protective coatings for steel panels [30]. The CA-PDMS could be crosslinked under the radiation of UV-light or sunlight and became viscoelastic so that the coating system has the repeatable self-healing ability.

Herein, we report a facile microencapsulation approach for a UV-curable self-healing system consisting of aliphatic polyurethane acrylate, 1,6-hexanediol diacrylate (reactive diluents) and 2-hydroxy-2-methyl-1-phenyl-1-propanone (photoinitiator 1173). The advantages of this healing system include the high flowability of encapsulated components in the damaged region and the excellent mechanical properties of the UV-cured healant such as the high impact and tensile strength, better abrasion resistance and toughness, as well as the good resistance to chemicals and solvents [31, 32]. The prepared microcapsules are embedded into green water-borne polyurethane (WPU) coatings, which can be cured under low temperature, and possess oil resistance, seawater resistance, wear resistance, impact resistance, *etc.* [33], to obtain an effective anti-corrosive protection film for copper.

II. EXPERIMENTS

A. Materials

Urea (CP), aqueous formaldehyde solution (37wt%), resorcinol (CP), 1-octanol (CP), and sodium dodecyl benzene sulfonate (SDBS, CP) were supplied by Shanghai Chemical Reagents Co. Ltd. EB270 (an aliphatic polyurethane acrylate with an unsaturation of 1.33 mmol/g and a mole mass of 1.5 g/mol) and 1,6-hexamethyl-diol diacrylate (HDDA) were supplied by Cytec Industries Inc. (USA). 2-hydroxy-2-methyl-1-phenylpropan-1-one (photoinitiator 1173) was provided by Runtec Chemical Co., Changzhou (China). Ammonium chloride, concentrated hydrochloric acid (37.5wt%), triethanolamine (TEA, 99.9%), acetone and copper foil (99.9%, Bi<0.1wt%, Sb<0.2wt%, Ca<0.2wt%, Cd<0.2wt%, Cl<0.1wt%, Cr<0.2wt%) were purchased from Shanghai Chemical Reagents Co. Ltd. Distilled water was used in all experiments.

B. Preparation of poly(urea-formaldehyde) microcapsules encapsulating UV-curable healing agents

The fabrication of PUF microcapsules via *in situ* polymerization in an oil-in-water (O/W) emulsion has been reported in Ref.[18]. In a brief, the monomer mixture of urea (10 g) and formaldehyde solution (26 g) was added into a 100 mL four-necked flask equipped with a condenser, a stirrer and a thermometer. The pH value of the solution was adjusted about 8 by dropping a certain amount of triethanolamine. The solution was kept at 70 °C for 1 h to form hydroxymethylurea. Then double volume of water was added into the system. A certain amount of the above reacted solution was mixed with 70 mL of aqueous solution containing SDBS (0.1 g), ammonium chloride (0.25 g) and resorcinol (0.25 g). EB270 (4 g), HDDA (6 g), and photoinitiator 1173 (0.4 g) were added into the solution under mechanical stirring to form an O/W emulsion. The agitation speed was 200, 400, 600, or 800 r/min respectively. One or two drops of 1-octanol were added to eliminate surface bubbles. After the emulsion was agitated at 25 °C for 1 h, the temperature was raised to 60 °C at a rate of 0.5 °C/min. Simultaneously, the pH of the reaction mixture was adjusted to 4 within 90 min by dropping dilute hydrochloric acid. After the reaction continued for 3 h, the mixture was cooled to room temperature. The products were collected by vacuum filtration, and washed with water and acetone for three times, then dried under vacuum at 45 °C for 24 h.

The fabrication of pure PUF resin for control samples followed the above steps under the agitation speed of 600 r/min.

C. Characterization of the encapsulation percent and the yield of the prepared microcapsules

The amount of encapsulated content in microcapsules was determined by the weighing method. The as-prepared microcapsules of a known weight ($W_{\rm ic}$) were crushed using pestle in mortar and transferred into a centrifuge tube (50 mL). The pestle and mortar were rinsed with acetone and the scrubbing washing solution was poured into the centrifuge tube. After standing for 72 h, the remained material was isolated by vacuum filtration and dried under vacuum at 45 °C for 24 h. The final weight of the remained material ($W_{\rm rc}$) was recorded. The encapsulation percent x of the prepareded capsules can be calculated according to the following equation:

$$x=\frac{W_{\rm ic}-W_{\rm rc}}{W_{\rm ic}}\times 100\% \qquad (1)$$

The yield y of the prepared microencapsules is calculated simply as below:

$$y=\frac{W_{\rm cap}}{W_{\rm core}+W_{\rm mon}}\times 100\% \qquad (2)$$

where $W_{\rm cap}$ is the mass of the collected microcapsules after drying, $W_{\rm core}$ is the feed dosage of EB270, HDDA, and photoinitiator 1173, and $W_{\rm mon}$ is the dosage of urea and formaldehyde.

DOI:10.1063/1674-0068/27/05/607-615

D. Characterization of the photoreaction conversion of encapsulated components

The mixture of EB270, HDDA, and photoinitiator 1173 was coated on a KBr disk and radiated with medium pressure mercury lamp (Fusion F300S-6, 310−1000 nm). The photoreaction conversion was measured by the ratios of the integrate areas of the two absorption bands in FT-IR spectra (1635 cm^{-1} for $\nu_{C=C}$ and 1525 cm^{-1} for the bending vibration of N−H as an internal standard) before and after the exposure.

E. Preparation of self-healing anticorrosion coatings

The WPU emulsion for the subsequent dip-coating or spin-coating of the cleaned copper substrates was prepared through our previously reported method [34]. The concentration of self-healing microcapsules in WPU emulsion was used as 10, 20, 30, and 40 mg/mL.

F. Morphological characterization and other properties

The morphologies of the prepared microcapsules and coatings surface were observed by optical microscopy (OM, Leica DM 1000) and field-emission scanning electron microscopy (FESEM, JEOL JSM-6700, 5 kV). Samples for OM were prepared by placing a drop of dispersed solution of microcapsules or WPU emulsion onto glass slides. For FESEM analysis, a drop of dispersed solution of microcapsules or WPU emulsion was placed onto a copper flake and dried in air at room temperature.

The static contact angle of water on the WPU coating was measured with a Contact Angle Meter SL200B (Solon Tech. Co., Ltd.). A droplet of water (2 μL) was injected onto the film. The water contact angle was recorded by special software (CAST 2.0). For each set of experimental conditions, three specimens were analyzed. The mean value was taken as the final result. The deviation of the measured contact angles between various specimens was less than 2°.

The infrared spectra of samples were obtained from a Bruker EQUINOX 55 Fourier transform infrared (FT-IR) spectrophotometer. The samples were mixed with potassium bromide (KBr) and pressed into pellets.

Electrochemical impedance spectroscopy (EIS) and Tafel analysis measurements were carried out by the CHI660 electrochemical workstation system (CHI Co. USA). The sample substrates (2.5 cm×2.5 cm) were placed into cells so that 4.5 cm^2 of the coated metal surface was exposed to corrosive solution (0.1 mol/L NaCl solution, 20 mL) at room temperature. Both the reference (saturated calomel) and counter (platinum) electrodes were immersed into the corrosive solution, and leads were attached to a clean area of the metal substrate, which served as the working electrode (copper). EIS measurements were performed for samples of both scratched and unscratched coating systems. The working electrode was coated with WPU film using a spin coater at a low speed of 500 r/min for 10 s and 1000 r/min for another 30 s. Then samples were dried at room temperature for 12 h. EIS measurements were operated at a constant potential of 1 V and a frequency varying from 10^5 Hz to 0.01 Hz. ZSimpWin software was adopted for data fitting of the experimental impedance.

TABLE I Parameters of PUF microcapsules prepared at different agitation speed.

Agitation speed/(r/min)	Mean size/μm	y/%	x/%
200	663	3.65	37.00
400	499	69.40	78.92
600	118	65.23	97.52
800		35.17	

Several samples were scratched with a sharp knife-edge crosswise on the metal surface (the width of scratches: 20−50 μm) immediately before measurement. The scratched samples were immersed in 0.1 mol/L NaCl solution at room temperature for 2 h.

III. RESULTS AND DISCUSSION

A. Preparation of PUF microcapsules loaded with UV-curable healing agents

The mechanism of the microencapsulation of a mixture of EB270, HDDA and photoinitiator 1173 (10:15:1 by mass) in a PUF shell is illustrated in Scheme 1.

It is well-known that the synthesis of PUF resin includes two steps: (i) formation hydroxymethylurea under alkaline condition, and (ii) hydroxymethylurea condenses to form macromolecules by the dehydration at an acidic condition [18]. In the (ii) step, a UV-curable healing system was added into the aqueous reaction solution to form oil droplets so that the cross-linked PUF *in situ* polymerized in water would precipitate on the surface of the oil droplets, forming a PUF shell. Finally, a PUF microcapsules loaded with UV-curable healing system were obtained. It is noted that the agitation speed in the second step depicted in Scheme 1 had a great influence on the yield and morphology of the final PUF microcapsules. The yields of the microcapsules changed with the agitation speed, as listed in Table I. The highest yield of the microcapsules can be achieved at a moderate agitation speed (400 r/min). OM images of microcapsules prepared at different agitation speed are shown in Fig.1. As the agitation speed decreased from 600 r/min to 200 r/min, the average diameter of the capsules increased from 118 μm to 663 μm (also listed in Table I). If the agitation was too vigorous, *e.g.* 800 r/min, most of microcapsule would be ruptured un-

DOI:10.1063/1674-0068/27/05/607-615

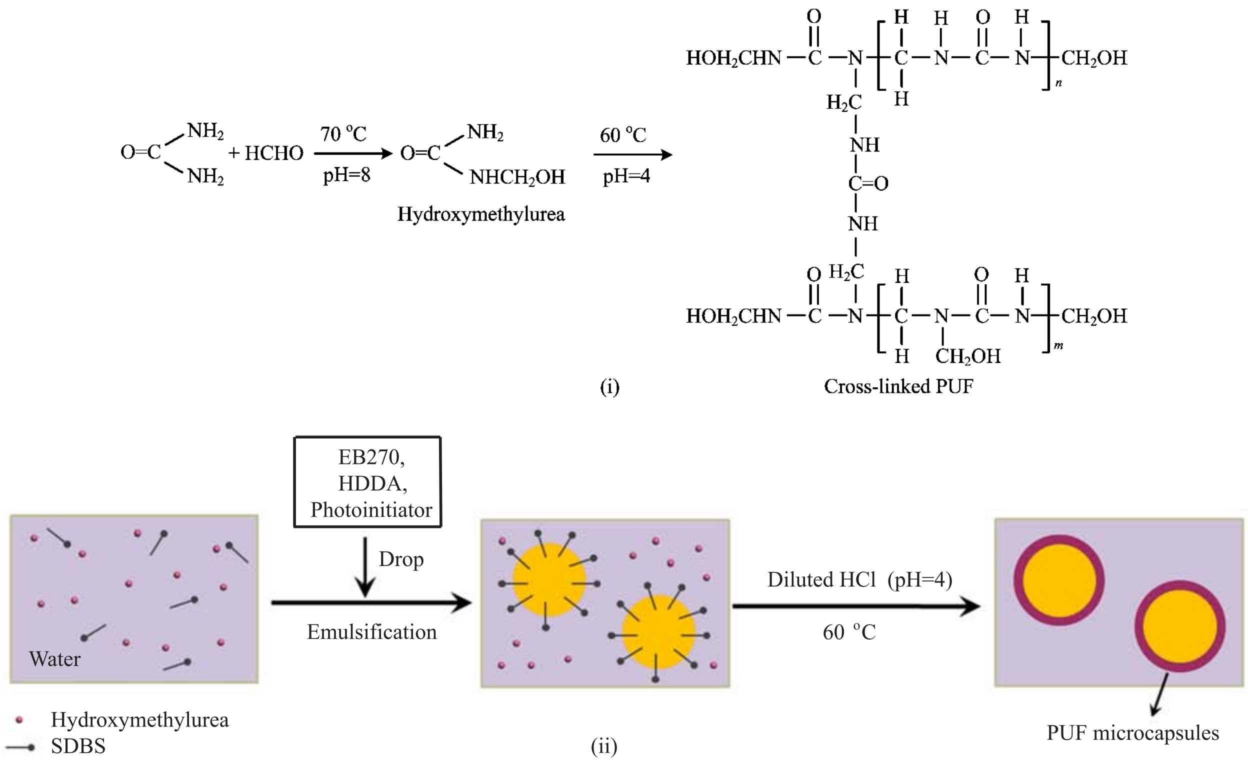

Scheme 1 The preparation process of PUF microcapsules loaded with UV-curable healing agents. (i) The synthesis of hydroxymethylurea and the cross-linked PUF through the condensation polymerization of hydroxymethylurea. (ii) The formation of PUF shell and the encapsulation of EB270, HDDA, and photoinitiator 1173.

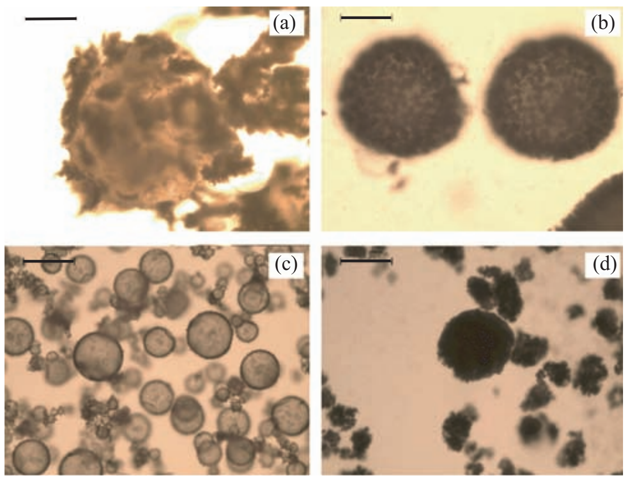

FIG. 1 OM images of microcapsules prepared at different agitation speeds in the second synthesis step. (a) 200 r/min, (b) 400 r/min, (c) 600 r/min, and (d) 800 r/min. The scale bar is 200 μm.

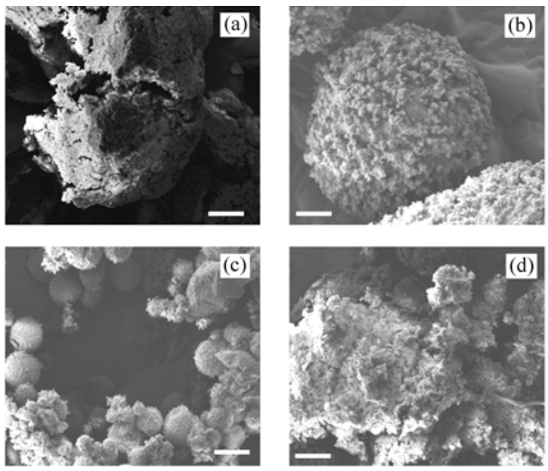

FIG. 2 SEM images of microcapsules prepared at different agitation speeds in the second synthesis step. (a) 200 r/min, (b) 400 r/min, (c) 600 r/min, and (d) 800 r/min. The scale bar is 100 μm.

der a high shear force (see Fig.1(d)) so that no effective encapsulation percent could be obtained (see Table I). The highest encapsulation percent of 97.52% could be achieved at an agitation speed of 600 r/min.

From the SEM images (Fig.2), it can be further confirmed that the microcapsules prepared at an agitation speed of 200, 400, and 600 r/min respectively were spherical in shape and rough on the shell. The rough morphology of microcapsules ensures the good mechanical bonding to coating matrix [26]. In a word, the agitation speed of 600 r/min is the most appropriate con-

DOI:10.1063/1674-0068/27/05/607-615

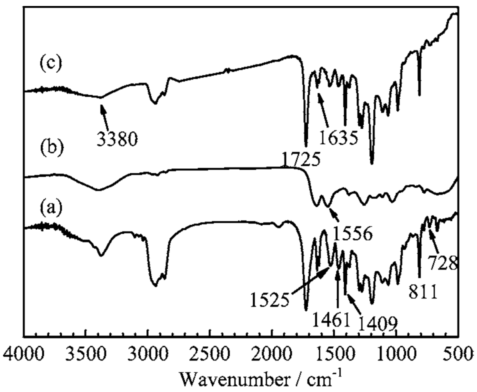

FIG. 3 FT-IR spectra of (a) the mixture of EB270, HDDA, and photoinitiator 1173, (b) pure PUF resin, and (c) PUF microcapsules loaded with of EB270, HDDA, and photoinitiator 1173.

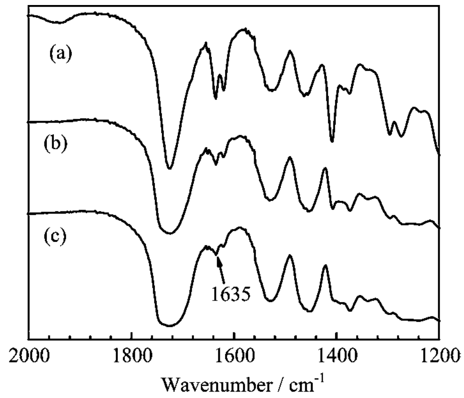

FIG. 4 FT-IR spectra of healing agents (EB270, HDDA, and photoinitiator 1173) radiated by medium pressure mercury lamp for (a) 0 s, (b) 10 s, and (c) 30 s.

dition for the preparation of the microcapsules loaded with those self-healing agents considering the yield, encapsulation percent, the particle size, and size uniformity. Therefore, the microcapsules obtained at an agitation speed of 600 r/min were adopted during the subsequent research.

The formation of microcapsules containing UV-curable healing system can be proven by FT-IR spectroscopy. As shown in Fig.3, the pure PUF shows the absorption peaks of $\nu_{\mathrm{N-H}}$ and $\nu_{\mathrm{O-H}}$ at 3380 cm^{-1}, $\delta_{\mathrm{N-H}}$ at 1525 cm^{-1}, $\nu_{\mathrm{C-N}}$ stretching vibration at 1556 cm^{-1}, and $\nu_{\mathrm{C=O}}$ at 1648 cm^{-1}. From Fig.3(c), the absorption peak at 1725 cm^{-1} can be assigned to the stretching vibration of carbamate C=O from EB270. The characteristic absorption peaks of C=C in acrylate units of EB270 and HDDA were located at 1635 cm^{-1}. The clear characteristic absorption peaks of benzene ring imply the encapsulation of photoinitiator 1173 cm^{-1} (1409 and 1461 cm^{-1} for benzene ring vibrations, 728 and 811 cm^{-1} for the benzene ring flexural vibrations). The results prove that EB270, HDDA, and photoinitiator 1173 have been encapsulated in PUF microcapsules. Moreover, the mixture of EB270, HDDA and photoinitiator 1173 was coated onto the KBr disk. It was found that the relative strength of the absorption peaks (1635 cm^{-1}) of C=C decreased with UV radiation time under medium pressure mercury lamp (see Fig.4). The absorption strength of C=C bonds relating to that of N−H bonds can be decreased sharply after 30 s of UV irradiation. It was indicated that the diacrylate units of EB270 and HDDA underwent polymerization reaction quickly.

B. Self-healing properties of WPU film embedded with PUF microcapsules loaded with UV-curable healing agents

The pure WPU coatings subjected to mechanical damage generally can be able to repair themselves. The self-healing efficiency can be promoted if the coatings are mixed with the active microcapsules containing healing agents. As shown in Fig.5, the PUF microcapsules could be well dispersed in the prepared WPU latex with the help of the emulsifier remaining on the surface of the PUF microcapsules and the polar interaction between the amide groups on the microcapsules and the carbamate groups of PU molecular chains.

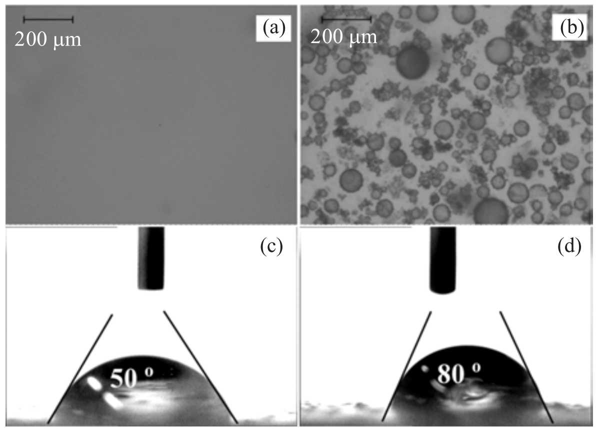

FIG. 5 The OM images and the water contact angle of WPU film embedded (a, c) without microcapsules and (b, d) with a 40 mg/mL mass concentration of microcapsules in the WPU emulsion.

The wettability of the WPU coating on a glass substrate was characterized by the contact angle instrument. The water contact angle on the pure WPU film (see Fig.5(c)) was only 50° because the main chains of WPU molecules possess some groups with strong affinity to water. This means that although the WPU film plays a role of physical barrier to corrosive agent, it is unable to completely prevent water from entering the gap between the film and the metal substrate. However, if the WPU latex is mixed with the prepared PUF microcapsules, the contact angle of the composite WPU film increases with the mass concentration of microcapsules in the coatings (see Fig.6). It was indicated that

DOI:10.1063/1674-0068/27/05/607-615

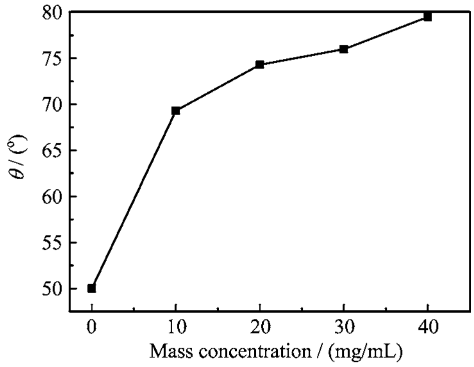

FIG. 6 The change of the water contact angle of composite WPU film with the different mass concentration of the embedded microcapsules.

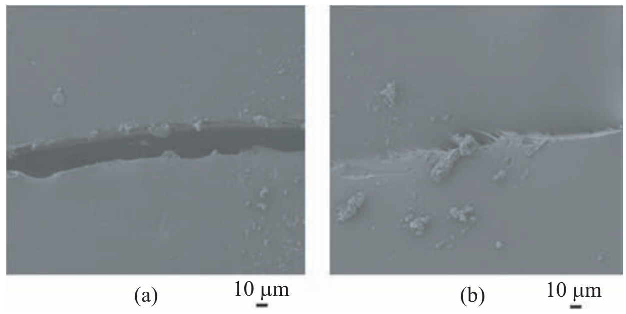

FIG. 7 SEM images of the scribed region of (a) pure WPU film and (b) WPU film embedded with the prepared PUF microcapsules radiated by UV light.

the addition of the prepared PUF microcapsules was beneficial to improve the waterproof and anticorrosion performance of coatings due to the rough surface of microcapsules (see Fig.2(c)).

The UV-curable healing agents loaded in the PUF microcapsules were integrated into the WPU latex at a mass concentration of 40 mg/mL. The WPU mixture was introduced onto a copper sheet and dried under ambient conditions for 24 h. It was demonstrated by SEM images that when the composite WPU coating was scratched with a cutter blade (see Fig.7(a)), the loaded healing agents could be released and cured rapidly in the scribed region under UV light for 30 s (see Fig.7(b)). The reason is the radical polymerization of prepolymer EB270 and reactive diluents is rapidly initiated by the free radicals generated from the cleavage of photoinitiator 1173 induced by the radiation of UV light so as to form a cured water-insoluble polyurethane film in the scribed regions.

C. Anticorrosive properties of WPU film embedded with PUF microcapsules loaded with healing agents

The electrochemical measurements of the anticorrosive WPU coatings with PUF microcapsules were performed by immersing samples in 0.1 mol/L NaCl solution. Figure 8 shows the electrochemical impedance spectra of the copper electrode coated with the pure WPU film and the WPU film embedded with the prepared microcapsules, as well as the bare Cu substrate. The low frequency impedance is the main parameter which gives the direct comparison of the corrosion protection efficiency of different coating systems. The higher impedance in the low frequency region suggests a lower corrosion activity on the copper surface. When the coating on the electrode is intact, the low frequency impedance of the copper protected by WPU film embedded with the PUF microcapsules is significantly higher than that coated by pure WPU film due to the better waterproof properties of the former (see Fig.5(d)).

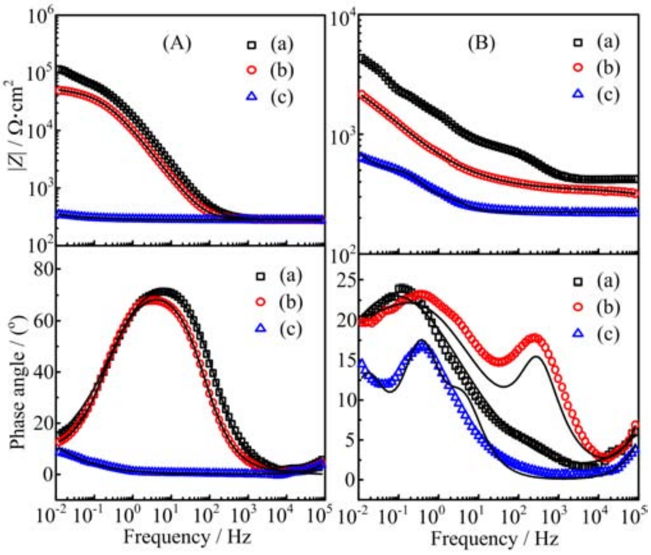

FIG. 8 Bode plots for copper electrode coated with (a) WPU film containing the microcapsules with UV-curable healing agents, (b) pure WPU film, and (c) no coating. The copper electrodes were immersed in 0.1 mol/L NaCl solution for 2 h before (A) and after (B) these electrodes were scratched by the blade and radiated by UV light. The solid lines are the fitting results.

In order to investigate the self-healing and corrosion resistance properties of the composited WPU coating, cross-cut was made on the coating surface of a sample by a razor blade. After one-hour's standing at ambient conditions and 30 s exposure under UV light, the samples were re-immersed in 0.1 mol/L NaCl solution for 2 h. The bare copper and copper coated with pure WPU coatings were also scratched and photoirradiated. The low frequency impedance of all samples decreased comparison with those of the unscratched samples because the corrosion species are prone to contact with the scribed metals. The copper coated with WPU film mixed with microcapsules showed the highest impedance at 0.01 Hz among three copper electrodes before or after these electrodes were scratched by the blade (see Fig.8).

DOI:10.1063/1674-0068/27/05/607-615

TABLE II The equivalent circuit elements for different samples, which were obtained by fitting the experimental impedance data[a].

	Original samples			Scratched samples[b]		
	A	B	C	A	B	C
$R_s/10^2\Omega\cdot cm^2$	2.20	2.51	2.85	2.28	4.12	1.43
$C/10^{-7}$ F	0.99			8350		
$R_t/10^2\Omega\cdot cm^2$	1.93	496	788	0.61	45.80	152
$W/(10^{-4}$ ms/cm$^2)$	411	4.97	0.13	128	8.49	3.04
$R_{pore}/10^2\Omega\cdot cm^2$		0.35	35.20		1.43	3.42
$Q_{pore}/(10^{-6}$ µs/cm$^2)$		7.33	10.10		0.15	2.75
n_{pore}		0.58	0.88		0.60	0.94
$Q_{dl}/(10^{-5}$ µs/cm$^2)$		1.47	0.70		111	29.50
n_{dl}		0.90	0.26		0.43	0.16

[a] Sample A: Copper electrode without coating. Sample B: Copper electrode coated by pure WPU film. Sample C: Copper electrode coated by composite WPU film.
[b] The copper electrodes were immersed in 0.1 mol/L NaCl solution for 2 h after these electrodes were scratched by the blade and UV-irradiated.

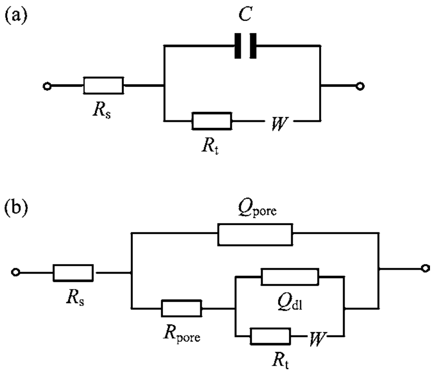

FIG. 9 Equivalent circuit representation for the copper electrode with (a) no coating and (b) coated by WPU with or without microcapsules. C is the capacitance, R_t is charge transfer resistance, R_s is solution resistance, R_{pore} is pore resistance of the coating, Q_{pore} is pseudo capacitance of the coating, W is Warburg impedance (contains mass transport limitations), Q_{dl} is the pseudo capacitance of the double layer.

The equivalent circuit and the equivalent circuit elements are represented in Fig.9 and Table II, respectively. The charge transfer resistance (R_t) is related to the kinetics of an electrochemical reaction at the interface, and can be reversely related to the corrosion rate. The pore resistance (R_{pore}) is related to the presence of pores and cracks in the polymeric coating and can reflect the barrier properties of the polymeric layer. The R_t value for copper electrode coated with WPU film containing the microcapsules is higher than pure WPU film when the coating was unscratched, which is attributed to the waterproof properties of the incorporated PUF microcapsules (see Fig.5(d)). After the coating was scratched, the value for the sample coated with WPU film containing the microcapsules is almost 3 times higher than that coated with pure WPU film, indicating the self-healing capacity of the microcapsules containing UV-curable healing agents. Moreover, it is demonstrated that the unsmooth microcapsules can cause higher value of R_{pore} compared with the pure coating due to its improved adhesion to the surface.

The corrosion rate r and inhibition efficiency η of copper electrode coated by WPU films can be calculated from the corresponding Tafel curves shown in Fig.10, according to the following equations:

$$r = \frac{I_{corr}KM}{n\rho A} \tag{3}$$

$$\eta = \frac{I^0_{corr} - I_{corr}}{I^0_{corr}} \times 100\% \tag{4}$$

where I_{corr} is current density of tested copper electrode. I^0_{corr} is current density of copper electrode without coating. The corrosion rate constant K is 327.2/(A·year). M is the molar mass of copper, 63.55 g/mol. n is 2, the transferred electron number in the corrosion reaction. The material density ρ=8.94 g/cm^3 for Cu [35]. The sample area A in this experiment is 4.5 cm^2.

The I_{corr} measured in NaCl solution showed again that the WPU film containing microcapsules had the best corrosion resistance among the investigated samples, although the linear range for some anodic or cathodic branches in our experimental conditions seemed still small, which might be related to the slow mass transfer in the solutions due to the slow magnetic agitation. The corresponding corrosion rate and inhibition efficiency are listed in Table III. The copper electrodes were immersed in 0.1 mol/L NaCl solution after these electrodes were scribed by the blade and radiated by UV light. The inhibition efficiency of WPU film mixed with the microcapsules almost triples that of the pure WPU film. All these results indicate that the combination of hydrophobic microcapsules and the released

DOI:10.1063/1674-0068/27/05/607-615

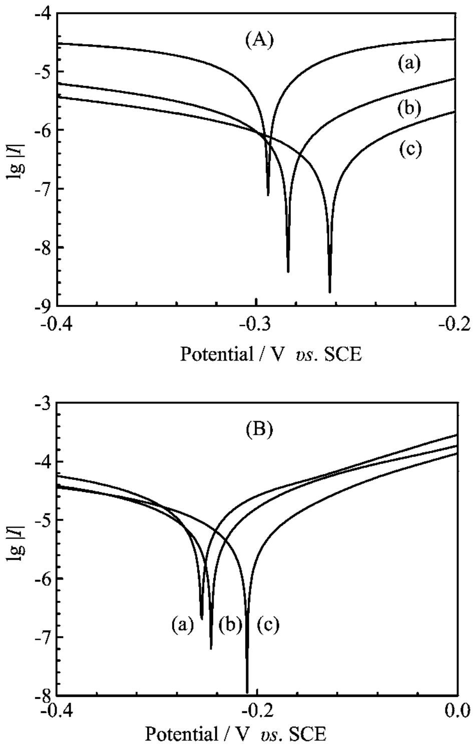

FIG. 10 Tafel plots for copper electrode covered by (a) no coating, (b) pure WPU film, and (c) WPU film containing the microcapsules with UV-curable healing agents. The copper electrodes were immersed in 0.1 mol/L NaCl solution for 2 h before (A) or after (B) these electrodes were scratched.

UV-curable healing agents can effectively increase the corrosion resistance of the scribed regions.

IV. CONCLUSION

In this work, a facile procedure for microencapsulation of UV-curable healing agents was achieved through an *in situ* condensation of hydroxymethylurea in water and precipitation at an oil droplets surface. Spherical microcapsules with the mean diameter in the range of 118 μm to 663 μm were prepared depending on the agitation speed from 600 r/min to 200 r/min during the condensation process. The yield and encapsulation percent of the microcapsules in this method can reach 97.52wt% and 65.23wt%, respectively at an agitation speed of 600 r/min.

Microcapsules incorporated WPU coating on a copper substrate showed good corrosion protection under an accelerated corrosion process via a mechanism of fast UV curing of the released core materials. The anticorrosive properties of the pure WPU film and the microcapsules incorporated WPU film were investigated by electrochemical measurement performed using electrochemical impedance spectroscopy and Tafel analysis. Whether the coatings were damaged or not, the anticorrosion efficiency of WPU film embedded with microcapsules was the best. This should be attributed to the combination of better hydrophobility and the loaded UV-curable healing system in the microcapsules. This work offers a practical way in the development of catalyst-free, one-part self-healing coatings for corrosion control.

TABLE III Corrosion rate r and inhibition efficiency η of different samples calculated from Tafel curves[a].

Sample	$r^b/(10^{-14}$ m/s)	η/%
Original		
A	87.50±0.02	
B	8.63±0.29	90.13
C	0.25±1.80	99.74
Scratched		
A	10.50±0.72	
B	7.39±0.42	15.54
C	4.41±1.50	49.60

[a] Sample A: Copper electrode without coating. Sample B: Copper electrode coated with pure WPU film. Sample C: Copper electrode coated with WPU film containing the microcapsules with UV-curable healing agents.
[b] The corrosion rates were obtained through averaging over five different samples.

V. ACKNOWLEDGMENTS

This work was supported by the National Natural Science Foundation of China (No.51173175, No.51073146, No.51103143, and No.51473152) and the Foshan Scientific and Technological Innovation Team Project (No.2013IT100041).

[1] D. G. Shchukin, S. V. Lamaka, K. A. Yasakau, M. L. Zheludkevich, M. G. S. Ferreira, and H. Möhwald, J. Phys. Chem. C **112**, 958 (2008).
[2] V. Palanivel, Y. Huang, and W. J. van Ooij, Prog. Org. Coat. **53**, 153 (2005).
[3] D. Raps, T. Hack, J. Wehr, M. L. Zheludkevich, A. C. Bastos, M. G. S. Ferreira, and O. Nuyken, Corros. Sci. **51**, 1012 (2009).
[4] M. Garcia-Heras, A. Jimenez-Morales, B. Casal, J. C. Galvan, S. Radzki, and M. A. Villegas, J. Alloy Compd. **380**, 219 (2004).
[5] C. Dry, Compos. Struct. **35**, 263 (1996).
[6] A. Latnikova, D. Grigoriev, M. Schenderlein, H. Möhwald, and D. Shchukin, Soft. Matter **8**, 10837 (2012).
[7] J. J. Fu, T. Chen, M. D. Wang, N. W. Yang, S. N. Li, Y. Wang, and X. D. Liu, ACS. Nano. **7**, 11397 (2013).
[8] A. N. Ababneh, M. A. Sheban, and M. A. Abu-Dalo, J. Mater. Civil. Eng. **24**, 141 (2012).

DOI:10.1063/1674-0068/27/05/607-615

[9] D. Gopi, K. M. Govindaraju, V. C. A. Prakash, D. M. A. Sakila, and L. Kavitha, Corros. Sci. **51**, 2259 (2009).
[10] S. D. Bergman and F. Wudl, J. Mater. Chem. **18**, 41 (2008).
[11] M. D. Hager, P. Greil, C. Leyens, S. van der Zwaag, and U. S. Schubert, Adv. Mater. **22**, 5424 (2010).
[12] Y. Yang and M. W. Urban, Chem. Soc. Rev. **42**, 7446 (2013).
[13] B. J. Blaiszik, S. L. B. Kramer, S. C. Olugebefola, J. S. Moore, N. R. Sottos, and S. R. White, Annu. Rev. Mater. Res. **40**, 179 (2010).
[14] S. R. White, N. R. Sottos, P. H. Geubelle, J. S. Moore, M. R. Kessler, S. R. Sriram, E. N. Brown, and S. Viswanathan, Nature **409**, 794 (2001).
[15] M. W. Keller, S. R. White, and N. R. Sottos, Adv. Funct. Mater. **17**, 2399 (2007).
[16] D. S. Xiao, Y. C. Yuan, M. Z. Rong, and M. Q. Zhang, Polymer **50**, 2967 (2009).
[17] T. S. Coope, U. F. J. Mayer, D. F. Wass, R. S. Trask, and I. P. Bond, Adv. Funct. Mater. **21**, 4624 (2011).
[18] R. Tian, X. L. Fu, Y. D. Zheng, X. Liang, Q. L. Wang, Y. Ling, and B. S. Hou, J. Mater. Chem. **22**, 25437 (2012).
[19] D. Y. Zhu, M. Z. Rong, and M. Q. Zhang, Polymer **54**, 4227 (2013).
[20] M. G. Ahangari, A. Fereidoon, M. Jahanshahic, and N. Sharifi, Compos. Part B **56**, 450 (2014).
[21] E. Koh, S. Lee, J. Shin, and Y. W. Kim, Ind. Eng. Chem. Res. **52**, 15541 (2013).
[22] R. K. Hedaoo, P. P. Mahulikar, A. B. Chaudhari, S. D. Rajput, and V. V. Gite, Int. J. Polym. Mater. **63**, 352 (2014).
[23] M. X. Huang and J. L. Yang, J. Mater. Chem. **21**, 11123 (2011).
[24] M. X. Huang and J. L. Yang, Prog. Org. Coat. **77**, 168 (2014).
[25] C. Suryanarayana, K. C. Rao, and D. Kumar, Prog. Org. Coat. **63**, 72 (2008).
[26] M. Samadzadeh, S. H. Boura, M. Peikari, A. Ashrafi, and M. Kasiriha, Prog. Org. Coat. **70**, 383 (2011).
[27] R. S. Jadhav, D. G. Hundiwale, and P. P. Mahulikar, J. Appl. Polym. Sci. **119**, 2911 (2011).
[28] Y. K. Song, Y. H. Jo, Y. J. Lim, S. Y. Cho, H. C. Yu, B. C. Ryu, S. I. Lee, and C. M. Chung, ACS. Appl. Mater. Inter. **5**, 1378 (2013).
[29] J. L. Yang, M. W. Keller, J. S. Moore, S. R. White, and N. R. Sottos, Macromolecules **41**, 9650 (2008).
[30] Y. K. Song and C. M. Chung, Polym. Chem. **4**, 4940 (2013).
[31] C. Y. Bai, X. Y. Zhang, J. B. Dai, and W. H. Li, Prog. Org. Coat. **55**, 291 (2006).
[32] J. W. Xu, W. M. Pang, and W. F. Shi, Thin Solid Films **514**, 69 (2006).
[33] H. X. Pan and D. J. Chen, Eur. Polym. J. **43**, 3766 (2007).
[34] D. Zhao, M. Z. Wang, Y. F. Xu, Z. C. Zhang, and X. W. Ge, Surf. Coat. Tech. **238**, 15 (2014).
[35] D. Prasai, J. C. Tuberquia, R. R. Harl, G. K. Jennings, and K. I. Bolotin, ACS Nano **6**, 1102 (2012).

DOI:10.1063/1674-0068/27/05/607-615